Current-Sheet Velocity in a Coaxial Plasma Accelerator

T. N. LIE*
Catholic University of America, Washington, D.C.

Several factors which affect the velocity of the current-sheet in a coaxial plasma accelerator such as the insulator ablation, the radius ratio of the electrode, the species of gas and its pressure are examined experimentally and the results are compared with the theoretical predictions. It appears that the albation and possibly the degassing from the insulator wall provide severe velocity drag and the detailed observations closely support the physical model on the ablation proposed by Keck. In general, however, the experimental values do not agree with a previous theory for the ablation. The cause for the disagreement is due to the fact that the velocity relation used in the previous analysis fails to account for the radius ratio of the coaxial accelerator.

I. Introduction

THE propagation velocity of the current-sheet in a coaxial plasma accelerator is in general limited, i.e., the velocity does not increase beyond a certain value even if the total energy input to the accelerator is greatly increased. The velocity limitations of the current-sheet in a coaxial accelerator have been investigated by a number of authors previously. Thom et al.[1] suggested that a drag force associated with ions striking the cathode acts on the accelerating plasma. The velocity drag depends on the ion-electron partition of the current-sheet and also on the atomic weight of the ambient gas used. Keck[2] proposed that the velocity limitation observed in his magnetic annular shock tube may be due to insulator ablation. The ionized vapor of ablated material near the insulator wall provides the current path and the additional mass introduced by the vapor contributes as an inertial drag.

The former[1] drag is only significant in a case where a heavier gas such as argon or air is used as the working gas and is negligibly small with lighter gases. Therefore it does not account for the velocity limitation observed with lighter gases.[2] The velocity drag due to the insulator ablation, on the other hand, could be a serious one regardless of the working gas used if Keck's physical model on the ablation is relevant.

The ablation drag was treated analytically by Workman[3] using a steady flow model very similar to that of Keck. His results show that the ablation loss can be expressed with a single correlation parameter which specifies the magnetic piston velocity as a function of the total magnetic field, the initial gas density, and the ionization potential of the insulator material. However, the theory requires a thorough experimental check in order to be generally accepted.

In this report, first, the current-sheet velocities in two groups of coaxial plasma accelerators with refractory and nonrefractory insulators are compared in a wide variety of operating conditions, in order to confirm the existence of a velocity drag due to ablation. This has not been done previously to the best of our knowledge. Secondly, the primary ablation process predicted by Keck is examined using a magnetic probe, monochromators and an image converter camera. Thirdly, Workman's theory on the ablation loss is compared with the measurements obtained in this study. An analytical expression for the current-sheet velocity has also been examined experimentally by varying several parameters of the coaxial accelerator.

Presented as Paper 69-265 at the AIAA Electric Propulsion Conference, Williamsburg, Va., March 3–5, 1969; submitted March 7, 1969; revision received August 20, 1969. This study is supported by NASA Grant NGR-09-005-025. The author wishes to acknowledge experimental assistance given by J. T. Williams and helpful advice from E. A. McLean. The author is also indebted to C. C. Chang for his interest and support.

* Research Associate Professor, Department of Space Science and Applied Physics.

II. Velocity Drag due to Insulator Ablation

A. Accelerators and Experimental Arrangement

The dimensions of the coaxial plasma accelerators used in this investigation are listed in Table 1 and their schematic diagram is shown in Fig. 1. The three accelerators used differ only in the inner electrode diameters—the outer electrode diameter is kept the same. The length of the electrodes is 22 cm. Two slots, 1 mm wide and 15 cm long, are provided on the outer electrode along the accelerator axis for the optical measurement. The insulator which separates the two cylindrical electrodes at the accelerator breech has the shape of a flat circular disk with a hole at the center. The insulating materials used so far are lucite, mylar, alumina, pyrex, and vycor glass and these are easily interchanged by removing the inner electrode. The accelerator electrodes are enclosed by a vacuum chamber 9 in. in diam and 60 in. long which is made of Plexiglass. A 60 μF capacitor is charged to 10 kv and the discharge is initiated by triggering a vacuum spark switch.[4] The quarter cycle time of the discharge is about 3.5 μsec. The maximum discharge current with a 10 kv charging voltage is about 160 kamp. The accelerator is operated with a static filling rather than with an injection of propellant gas. The working gases used are hydrogen, helium, nitrogen, and argon in the pressure range of 0.03–1.5 torr. The base pressure of the vacuum chamber prior to the gas filling is always below 1 mtorr, and after each shot the chamber is evacuated and refilled to insure the purity of the gas.

Table 1 Dimensions of coaxial plasma accelerator

Accelerator	Diam of O.E., mm	Diam of I.E., mm	Insulator
7A	60	22	Mylar, Lucite, Pyrex and Vycor Glass
7B	60	32	Pyrex Glass, Lucite
7C	60	40	Lucite

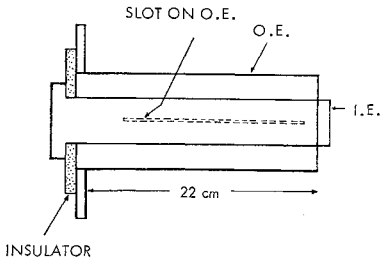

Fig. 1 Dimensions of the coaxial plasma accelerators (Table 1).

Most of the experimental measurements in the present investigation consist of accurate determinations of the luminous front velocity from streak photographs taken of the moving plasma through the slot in the outer electrode. An image converter streak camera is used for the photography. Since the velocity of the luminous front varies with time as the discharge current increases, the velocity measurements are made at a fixed phase or a fixed time of the discharge cycle rather than at a fixed position of the accelerator barrel. This is monitored by oscillograms of the discharge current and the image converter streak monitoring signal from the camera simultaneously. Figure 2 shows a typical streak photograph and oscillograms of the discharge current and the streak signal recorded simultaneously. As can be seen, the luminous front is usually well defined for the gas pressure range used in this investigation. The shot-to-shot reproducibility of the measurement is 10% or better in most cases. One notices bright second fronts in the photograph which have approximately the same velocity as first front. As already reported in a previous report,[5] the first and second front in the streak photograph correspond to the portions of the current-sheet which intersect with the inner and the outer electrode, respectively. The second front is usually brighter than the first front because this part of the current-sheet, along the outer electrode wall, forms a well-defined ring where the electron density is rather high.

B. Velocity Difference between the Accelerators with Refractory and Nonrefractory Insulators

In order to avoid further complications, the accelerator geometry is kept the same while the insulators are changed from one material to another for comparison. Four different insulator materials are used with Accelerator 7A and the sheet velocities are measured at fixed capacitor charging voltage. The result is shown in Fig. 3, where the measured velocities are plotted against the filling pressure of nitrogen and hydrogen. The velocities corresponding to the trials with insulator materials of lucite and mylar give approximately the same value in the pressure range used here. The velocities with vycor and pyrex glass are also very close to each other within the experimental scatter. However, one notices a large velocity difference between the two groups of insulators, i.e., velocities with a lucite insulator give about 65–70% of that with vycor glass. It should also be noted that all curves (regardless of the insulator material) follow approximately the snowplow prediction $U \propto \rho^{-4}$, where U and ρ are the measured velocity and the initial gas density, respectively.

C. Process of Insulator Wall Ablation

The velocity difference observed in the accelerator with refractory and nonrefractory insulators is almost certainly caused by the ablation from the insulator wall. Keck[2] has predicted that the inertial drag of material ablated from the walls is the main source of the velocity limitation in an accelerator where nonrefractory material is used. According to him, the ablation of the insulator wall takes place in the early stage of the discharge. The material from the wall is rapidly ionized and, since it is at rest in a strong electric field,

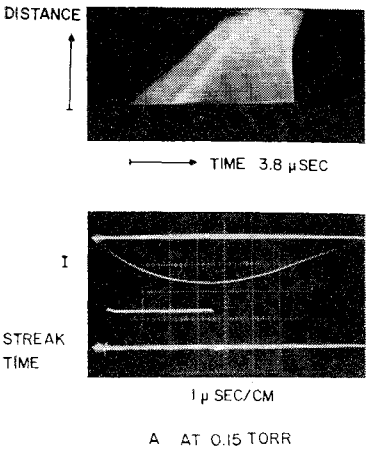

Fig. 2 Streak photograph of luminous front and simultaneous recording of total discharge current and streak monitor signal.

a current will flow, causing both joule heating and an acceleration of the ablated material. A well-confined standing arc is formed close to the insulator wall and in turn transfers a portion of its heat (or energy) back to the insulator end-wall, thus generating a continuous flow of vapor from the wall. Only a portion of the total discharge current would flow in the current-sheet under this circumstance, resulting in a reduction in the sheet velocity.

A qualitative check on Keck's ablation model is made experimentally. First, in order to examine the existence of ablated material flow behind the current-sheet, two monochromators are focused through the slots in the outer electrode at two separate axial locations of the accelerator barrel. The line of sight of both monochromators is perpendicular to the accelerator axis z. Among the probable impurities, the singly and doubly ionized carbon spectral lines seem to be the most intense lines behind the current-sheet when lucite is

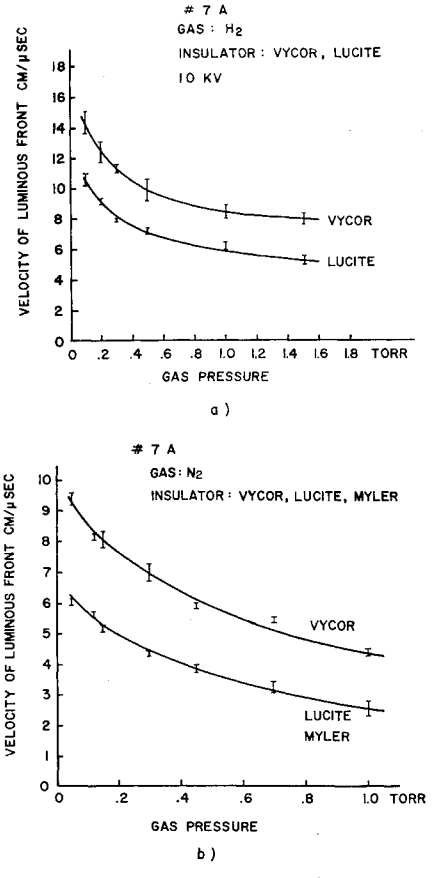

Fig. 3 Comparison of velocities in Accelerator 7A with refractory and nonrefractory insulator; a) with hydrogen gas and b) with nitrogen gas filling, respectively.

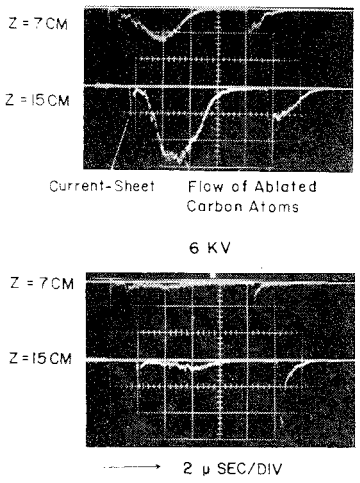

Fig. 4 Photoelectric signals of C II 4267 Å at $z = 7$ cm and $z = 15$ cm showing ablated material flow behind the current-sheet.

used as an insulator. Figure 4 shows typical photoelectric signals of the C II 4267Å line at $z = 7$ cm and $z = 15$ cm (insulator wall is at $z = 0$), respectively. As can be seen, the first arriving peak which is sharp and has a relatively low amplitude is followed by a high and broad second pulse. The initial carbon line signal coincides with the current-sheet and the second peak with the flow of ablated carbon atoms from the insulator. The propagation velocity of each pulse can be derived from the time delay as measured on the oscillogram. The flow velocity of the ablated material is found to be very close to that of the current-sheet. A similar recording with a 6 kv charging voltage shows the second peak to be very low in amplitude compared with the first peak, in contrast to the 10 kv case described previously. The third peak on the oscillogram is the current-sheet produced by a reversed discharge of the second half cycle.

In order to check the carbon ion formation near the insulator wall, a monochromator is focused so as to look primarily at a portion of the volume in the vicinity of the insulator wall. This is done by observing the plasma from the back of the accelerator through the insulating disk. The photoelectric signal of the C III 4647 Å line is shown in Fig. 5, where the discharge current waveforms are also recorded. The peaks of both C II and C III lines signals coincide with the discharge current maximum in time, and the amplitude of the signal is negligibly small at the beginning and the end part of the first half cycle. A comparison with 6 kv data indicates that far less ablation takes place at the lower discharge current.

The same spectroscopic observations are made with vycor glass used as an insulator. The carbon line signals appear to be negligibly small and do not form a distinct second peak when the system is clean. Possible silicon lines are also examined but these line signals are found to be very small. The same observations were made in an accelerator with an alumina insulator. The carbon impurity signal following the current-sheet was found as in the case with lucite. When the insulator disk was removed, it was found that the surface was covered with a black material, apparently carbon impurity. This is probably due to the fact that the surface of the material is not as smooth as that of glass and the deposit of impurity is built up shot after shot. The preceding ob-

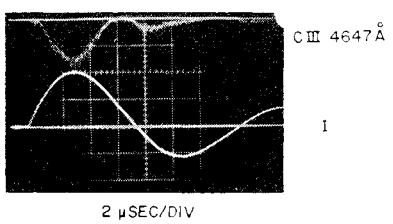

Fig. 5 Simultaneous recording of discharge current and photoelectric signals CIII 4247 Å observed in the vicinity of the insulator wall.

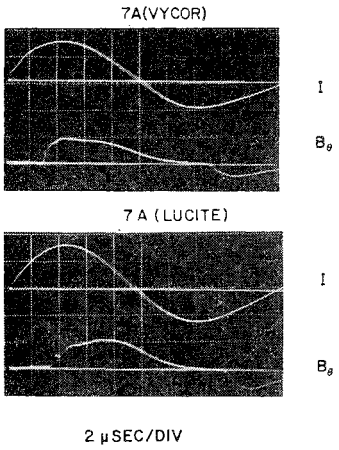

Fig. 6 Comparison of magnetic probe signal in Accelerator 7A with vycor glass and lucite insulator.

servations, although qualitative, confirm that the carbon impurities are produced as a result of insulator wall ablation and that the current sheet is followed by a flow of ablated material, apparently consisting of singly and doubly ionized carbon atoms. The impurity flow from the wall is maximum at the discharge current maximum and ceases to flow at the lower current, e.g., at the beginning and the end of the first cycle.

A magnetic probe is used to measure the azimuthal field B_θ in order to determine the proportion of current carried in the current-sheet. The integrated probe signals with lucite and vycor glass insulators are compared in Fig. 6. It is seen that the signal waveforms are different, i.e., the current carried in the current-sheet in the case of the lucite insulator is very small compared to the case of the vycor glass insulator and a considerable portion of the discharge current is conducted in the region behind the current-sheet, probably through the ablated material. Figure 7 shows the measured radial current in the annulus with two different capacitor charging voltages. In the 10 kv case, the current carried by the sheet is less than 50%, whereas about 80% of the total discharge current is carried in the case of 6 kv. This is as expected from the fact that far less ablation takes place with the low discharge current.

According to Keck's[2] model, a thin standing arc zone adjacent to the insulator wall exists. This is examined with frame photographs from an image converter camera taken of this region. For this, a parallel plate accelerator is used, allowing direct observation. The electrodes are separated by a lucite insulator and the gap is 3 cm. The quarter cycle time of the discharge is 2 μsec in this case. In Fig. 8, one can clearly see immediately adjacent to the insulator a discharge column which gets brighter near the current maximum

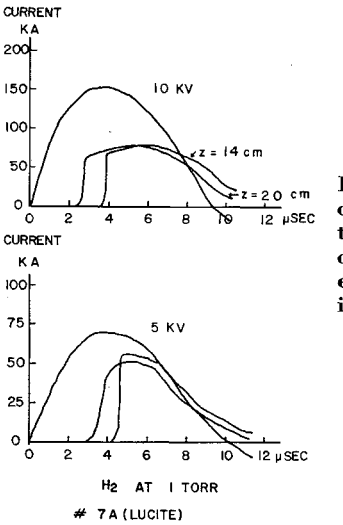

Fig. 7 Sketch of discharge current and integrated probe signals comparing two different charging voltages in Accelerator 7A (with lucite insulator).

Fig. 8 Framing photograph taken with a parallel plate accelerator showing standing arc in the vicinity of insulator wall.

in time and becomes dim thereafter. This supports the existence of a standing arc zone as predicted by Keck and the fact[2] that the ablation takes place as a result of energy transfer from the standing arc to the insulator wall, and the vaporized gas (possible mostly ionized) is accelerated by a Lorentz force in the arc. If the energy transfer is simply in the form of heat, the maximum temperature of the insulator wall may be in the order of 800°C.

D. Comparison with Workman's Theory

Workman[3] has developed a theory for the insulator ablation, which is based on the physical model proposed by Keck. The conclusion of the analysis is that the ratio of observed velocity U_p to the ideal velocity U_0 is determined by the parameter $\beta = 2\epsilon_I/(m_A \cdot U_0^2)$, where ϵ_I and m_A are, respectively, the ionization potential and the atomic weight of the insulator material. The vaporization energy of the insulator material is assumed to be negligible compared to the ionization energy. The ideal velocity U_0 is the velocity that corresponds to the case of no ablation and is related to the magnetic field B_0 and the initial density ρ_g by the Kemp and Petschek's[6] expression of $B_0^2/2\mu_0 = (\frac{4}{3})\rho_g U_0^2$, where $B_0 = \mu_0 I_0/2\pi r$.

Workman's result is examined experimentally under a wide variety of conditions of accelerator operations. Figure 9 illustrates the comparison between the theory and the experimental data. The value of β is changed mainly by varying the initial gas density. One notices that all of the points deviate considerably from the theoretical curve but a set of U_p/U_0 values for each accelerator falls on a curve which is roughly parallel to the theoretical curve. This implies that Workman's analysis does not take into consideration the geometric effect, i.e., the radius ratio of the accelerator electrode. As can be seen in Fig. 9, the values of U_p/U_0 with 7C($r_2/r_1 = 1.5$) are generally much larger than that with 7A ($r_2/r_1 = 2.7$) for the same β. A similar result is also obtained using accelerators with a vycor glass insulator and therefore this is not related to insulator ablation.

According to the ideal velocity relation, $U_0 \propto B_0(r_1)$ and U_0 decreases as the radius of the inner electrode increases according to r_1^{-1}. The current-sheet velocity measurements with Accelerators 7A, 7B, and 7C, in which only the diameter of the inner electrode differ, is made to further clarify this problem. The charging voltage, species of gas, and initial gas density are kept the same and the same insulator material is used for the measurement. The result is shown in Fig. 10, where an arbitrary curve of r^{-1} is also shown for comparison. The measured values are off from the r_1^{-1} curve within the r_2,r_1 combination used here, i.e., the velocity decreases only slightly while the radius r_1 increased from 11 mm to 20 mm. It is apparent then that the disagreement between Workman's theory and the present experiment is due to the expression of the ideal velocity (Kemp and Petschek's) used in his analysis, which is not sufficient to reflect the geometric effect of a coaxial accelerator. There has been an analysis

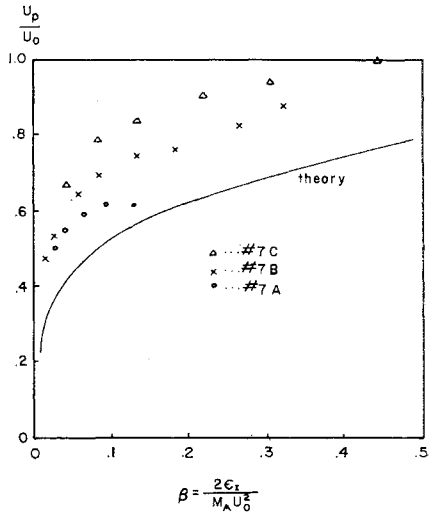

Fig. 9 Plot of velocity ratio U_p/U_0 against a parameter β showing comparison between the theory and measured values.

where the effect of radius ratio of a coaxial accelerator was included.[7]

III. Current-Sheet Velocity

A model of the current-sheet motion in a coaxial accelerator in which the geometry of the accelerator is better indicated may be obtained from a simplified analysis of the snowplow model. Considering the ratio of mass accumulation in the current-sheet, the equation of motion is expressed by

$$d/dt(mdz/dt) = (\tfrac{1}{2})I^2\,\partial L/\partial z \qquad (1)$$

and

$$L = L_0 + L'z$$

$$m = S\rho_0 z$$

where L_0 represents the parasitic inductance of the external circuit, $L' = 2\ln(r_2/r_1)$ the inductance per unit length of the electrode, $S = \pi(r_2^2 - r_1^2)$ the cross section of the accelerator annulus, and I, the discharge current. Equation (1) becomes

$$(S\rho_0/2)(d^2z^2/dt^2) = (L'/2)I^2 \qquad (2)$$

using $I = -CdV/dt$, $V = d/dt(L_0 + L' \cdot z)$I, and also taking two simplifying assumptions, i.e., the capacitor voltage V_0 to be constant during the acceleration and $L_0 \gg L' \cdot z$. The velocity of the current-sheet is then given by[8]

$$dz/dt = [4L'(V_0 \cdot z)^2/3S\rho_0 L_0^2]^{1/4} \qquad (3)$$

Although the preceding expression is not strictly quantitative due to the assumptions made, it gives a useful relation

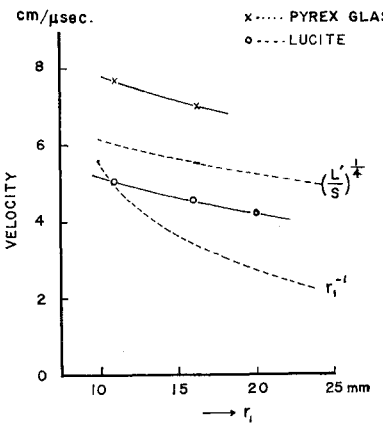

Fig. 10 Current-sheet velocity as a function of inner electrode radius r_1.

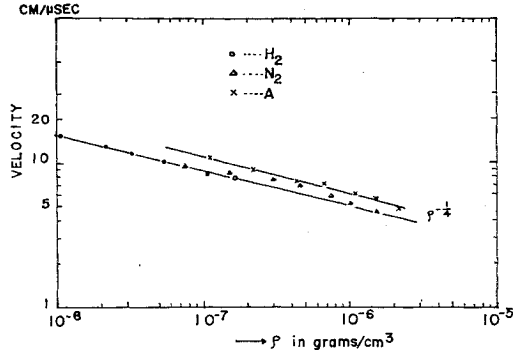

Fig. 11 Current-sheet velocity as a function of initial gas density.

for accelerator parameters such as L',S,ρ_0,z, and V_0. L' and S are determined from a combination of r_2 and r_1 in a coaxial accelerator. In Fig. 10, a curve of $(L'/S)^{1/4}$ is plotted and one sees the parametric agreement with the experimental velocities. Furthermore, the current-sheet velocities are plotted against initial gas density for hydrogen, nitrogen, and argon. As can be seen in Fig. 11 there exists a slight discrepancy[3] between the curves for hydrogen and argon; however, the measured points fall approximately on a $\rho^{-\frac{1}{4}}$ curve within the density range used here. The velocities are measured also by changing the charging voltage of the capacitor from 6 kv to 10 kv. The results show roughly $U \propto (V_0)^{1/2}$, in agreement with previous work.[9]

IV. Conclusion

A direct cause for the velocity drag in the coaxial plasma accelerator where nonrefractory material is used as an insulator is that the radial current in the current-sheet is very small, being only a fraction of the total discharge current. The mass flow of insulator wall material (mainly ionized carbon) which follows the accelerating current-sheet is observed. A thin standing arc adjacent to the insulator wall is also confirmed from the frame photographs taken in a parallel plate accelerator. The ablation process is therefore a result of energy transfer (e.g., heat) from the standing arc to the wall, and vaporized wall material is ionized and accelerated through the arc up to the sheet velocity. The flow rate of ablated gas from the wall sensitively depends on the total discharge current, or possibly the current through the standing arc. The experimental observations described previously support Keck's proposed model of the ablation process. Workman's analysis on the ablation is examined using the three accelerators.

The theory does not agree well with the experimental values and the cause for the failure is considered to be Kemp and Petschek's velocity relation used in the analysis which does not reflect the geometric effect of the accelerator. The velocity relation shown in Eq. (3) seems to agree with such parameter change as radii combinations of inner and outer electrodes, the initial gas density, and the charging voltage of the capacitor. However, it is obvious that such a simple snowplow relation does not account for the complex flow actually present, particularly due to the large current path through ablating insulator. Therefore, a further study is needed to develop a quantitative theory which combines the appropriate snowplow model with the ablation theory.

References

[1] Thom, K., Norwood, J., and Jalufka, N., "Velocity Limitation of a Coaxial Gun," *The Physics of Fluids*, Vol. 7, No. 11, Nov. 1964, pp. S67–S70.

[2] Keck, J., "Current Speed in a Magnetic Annular Shock Tube," *The Physics of Fluids*, Vol. 7, No. 11, Nov. 1964, pp. S16–S27.

[3] Workman, J. B., "Insulator Ablation in Magnetic Piston Shock Tubes," *The Physics of Fluids*, Vol. 8, No. 12, Dec. 1965, pp. 2162–2168.

[4] Mather, J. W. and Williams, A. H., "Some Properties of a Graded Vacuum Spark Gap," *The Review of Scientific Instruments*, Vol. 31, No. 3, March 1960, pp. 297–303.

[5] Lie, T. N. et al., "Plasma State in a Coaxial Accelerator," *The Physics of Fluids*, Vol. 10, No. 7, July 1967, pp. 1545–1552.

[6] Kemp, N. H. and Petschek, H. E., "Theory of the Flow in the Magnetic Annular Shock Tube," *The Physics of Fluids*, Vol. 2, No. 6, Nov.-Dec. 1959, pp. 599–608.

[7] Fishman, F. J. and Petschek, H., "Flow Model for Large Radius-Ratio Magnetic Annular Shock Tube Operation," *The Physics of Fluids*, Vol. 5, No. 5, May 1963, pp. 632–633.

[8] Artsimovich, L. A., *Controlled Thermonuclear Reaction*, Gordon and Breach, New York, 1964.

[9] Mather, J. W., "Formation of High Density Deuterium Plasma Focus," *The Physics of Fluids*, Vol. 8, No. 2, Feb. 1965, pp. 366–377.